Single-Gap s-Wave Superconductivity near the Charge-Density-Wave Quantum Critical Point in Cu_xTiSe_2

S. Y. Li,[1] G. Wu,[2] X. H. Chen,[2] and Louis Taillefer[1,3,*]

[1]*Département de physique and RQMP, Université de Sherbrooke, Sherbrooke J1K 2R1, Canada*
[2]*Hefei National Laboratory for Physical Science at Microscale and Department of Physics, University of Science and Technology of China, Hefei, Anhui 230026, People's Republic of China*
[3]*Canadian Institute for Advanced Research, Toronto M5G 1Z8, Canada*

(Received 26 January 2007; published 7 September 2007)

The in-plane thermal conductivity κ of the layered superconductor Cu_xTiSe_2 was measured down to temperatures as low as $T_c/40$, at $x = 0.06$ near where the charge-density-wave order vanishes. The absence of a residual linear term at $T \to 0$ is strong evidence for conventional s-wave superconductivity in this system. This is further supported by the slow magnetic field dependence, also consistent with a single gap, of uniform magnitude across the Fermi surface. Comparison with the closely related material $NbSe_2$, where the superconducting gap is 3 times larger on the Nb $4d$ band than on the Se $4p$ band, suggests that in $Cu_{0.06}TiSe_2$ the Se $4p$ band is below the Fermi level and Cu doping into the Ti $3d$ band is responsible for the superconductivity.

DOI: 10.1103/PhysRevLett.99.107001 PACS numbers: 74.25.Fy, 74.25.Jb, 74.25.Op

Superconductivity has recently been found in the layered compound $TiSe_2$, when its charge-density-wave (CDW) transition is continuously suppressed by Cu doping [1]. The phase diagram of Cu_xTiSe_2 is illustrated in Fig. 1, where superconductivity (SC) emerges near $x = 0.04$ and reaches a maximum T_c of 4.15 K at $x = 0.08$, beyond which T_c decreases [1]. Such a phase diagram is reminiscent of high-T_c cuprates and some heavy fermion (HF) superconductors, in which SC appears close to where magnetic order disappears with doping or pressure. For comparison, the phase diagram of the HF antiferromagnet $CeIn_3$ [2] is reproduced in Fig. 1.

The fact that superconductivity emerges precisely at the quantum critical point (QCP) where antiferromagnetic order vanishes in $CeIn_3$ and $CePd_2Si_2$ has been viewed as a compelling argument that this superconductivity is mediated by magnetic fluctuations [2]. Similarly, valence fluctuations were suggested to mediate the superconductivity in $CeCu_2(Si_{1-x}Ge_x)_2$, a HF system with a valence transition induced by pressure [3]. Theoretically, Monthoux and Lonzarich have recently shown that density fluctuations can mediate superconductivity and find that a d-wave order parameter is favored [4]. However, in none of the QCP-related superconductivity of HF materials is the symmetry of the order parameter known. In this context, the occurrence of superconductivity in Cu_xTiSe_2 near its CDW QCP is of great interest, particularly as we are able to investigate the symmetry of the order parameter by checking if there are nodes in the superconducting gap.

Layered dichalcogenides MX_2 (M = transition metal, X = S, Se, or Te) come in two structures: $1T$ or $2H$. Both $1T$ and $2H$ structures consist of two-dimensional X-M-X layers in which the X atom sheets exhibit a hexagonal close-packed structure and the M atoms are in octahedral ($1T$) or trigonal prismatic ($2H$) holes defined by the two X sheets. While CDW order has been well studied in both $1T$ and $2H$ structured MX_2 compounds [5–9], superconductivity was only seen in $2H$ structures, such as $2H$-$TaSe_2$, $2H$-TaS_2, $2H$-$NbSe_2$, and $2H$-NbS_2 [10]. Angle-resolved photoemission spectroscopy (ARPES) [11] and thermal conductivity [12] studies have revealed that $2H$-$NbSe_2$ ($T_c = 7.2$ K) is a multiband s-wave superconductor whereby the gap is large on one part of the Fermi surface and much smaller (3 times) on another part. By intercalating $1T$-$TiSe_2$ with Cu, Cu_xTiSe_2 is the first superconducting $1T$-structured MX_2 compound [1]. It is interesting to compare the superconducting ground states of $2H$-$NbSe_2$ and $1T$-Cu_xTiSe_2.

In this Letter, we probe the superconducting ground state of $Cu_{0.06}TiSe_2$ by measuring the thermal conductivity κ of

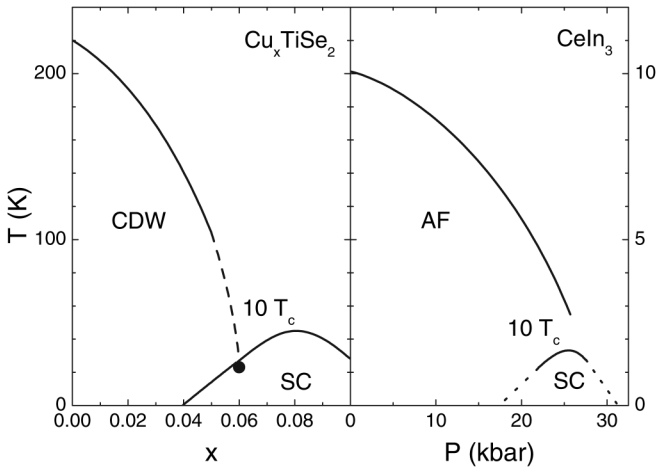

FIG. 1. Left: The $T - x$ electronic phase diagram of Cu_xTiSe_2 [1]. The closed circle represents the $Cu_{0.06}TiSe_2$ single crystal with $T_c = 2.3$ K used in this study. Right: Temperature-pressure phase diagram of the antiferromagnet $CeIn_3$ [2].

a single crystal down to 50 mK. This doping concentration is right at the critical point where the CDW order vanishes. In zero field, the residual linear term κ_0/T is zero, a clear indication that $Cu_{0.06}TiSe_2$ is an *s*-wave superconductor with a gap that is finite everywhere on the Fermi surface (no nodes). The field-dependence of κ_0/T shows conventional *s*-wave behavior, with no evidence for a variation of the gap magnitude across the Fermi surface, in contrast to the case of $NbSe_2$ where strong multiband character is observed. The difference is explained by examining the evolution in the band structure of Cu_xTiSe_2 upon Cu doping.

Single crystals of $Cu_{0.06}TiSe_2$ were grown by the vapor-transport technique [13]. The copper concentration was determined by inductively coupled plasma spectrometer (ICP) chemical analysis, and confirmed by *c* lattice parameter calibration [1]. The sample was cut to a rectangular shape of dimensions 1.5×1.0 mm^2 in the plane, with 30 μm thickness along the *c* axis. Contacts were made directly on the fresh sample surfaces with silver paint, which were used for both thermal conductivity and resistivity measurements. The typical contact resistance was 20 mΩ at low temperature. In-plane thermal conductivity was measured in a dilution refrigerator down to 50 mK using a standard one-heater–two-thermometer steady-state technique. Magnetic fields were applied along the *c* axis and perpendicular to the heat current.

Figure 2 shows the in-plane resistivity of our $Cu_{0.06}TiSe_2$ single crystal in $H = 0$ and 2 T. In zero field, the middle point of the resistive transition is at $T_c = 2.3$ K, in good agreement with previous studies [1]. The 10%–90% width of the resistive transition is 0.15 K, indicating the high homogeneity of our crystal. The normal-state resistivity in $H = 2$ T is essentially temperature independent below 0.5 K, which gives the residual resistivity $\rho_0 = 70.4\ \mu\Omega$ cm. This value is comparable to that of a $Cu_{0.07}TiSe_2$ single crystal [14]. The inset of Fig. 2 shows the field dependence of ρ at 80 mK, from which the upper critical field $H_{c2}(80\text{ mK}) \approx 0.52$ T is obtained. The normal-state magnetoresistance is negligible.

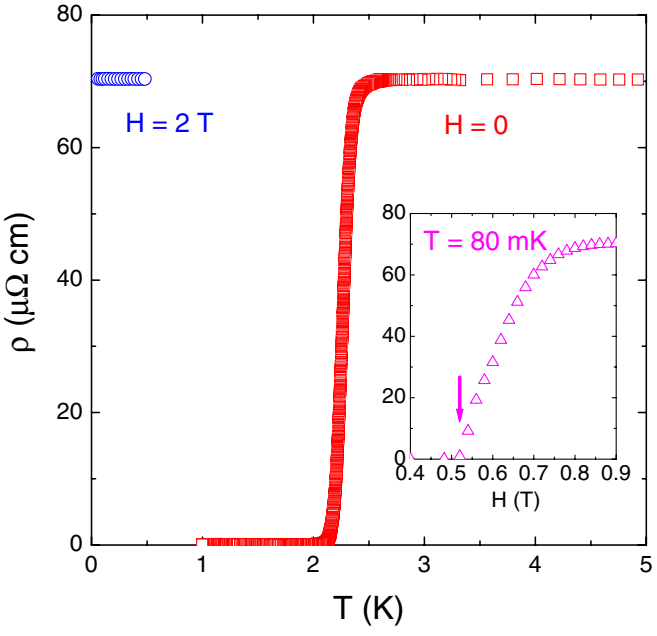

FIG. 2 (color online). In-plane resistivity for our $Cu_{0.06}TiSe_2$ single crystal in zero field and $H = 2$ T applied along the *c* axis. Inset: Field dependence of ρ at $T = 80$ mK, from which $H_{c2}(80\text{ mK}) \approx 0.52$ T is obtained (arrow).

The in-plane thermal conductivity of $Cu_{0.06}TiSe_2$ is plotted in Fig. 3(a), as κ/T vs T. By applying a magnetic field ($H > H_{c1} \sim 5$ mT [14]), a roughly rigid shift develops from the $H = 0$ curve and eventually saturates above $H = 0.55$ T. The measured conductivity is the sum of two contributions, respectively, from electrons and phonons, so that $\kappa = \kappa_e + \kappa_p$. In order to extract κ_e at $T \to 0$ we extrapolate κ/T to $T = 0$, i.e., obtain the residual linear term κ_0/T. This can be done by fitting the data to $\kappa/T = a + bT^{\alpha-1}$, below 150 mK. In the normal state of $H = 2$ T, this gives $\kappa_0/T = 0.355 \pm 0.016$ mW K^{-2} cm^{-1}, with $\alpha = 2.24$. This satisfies the Wiedemann-Franz law,

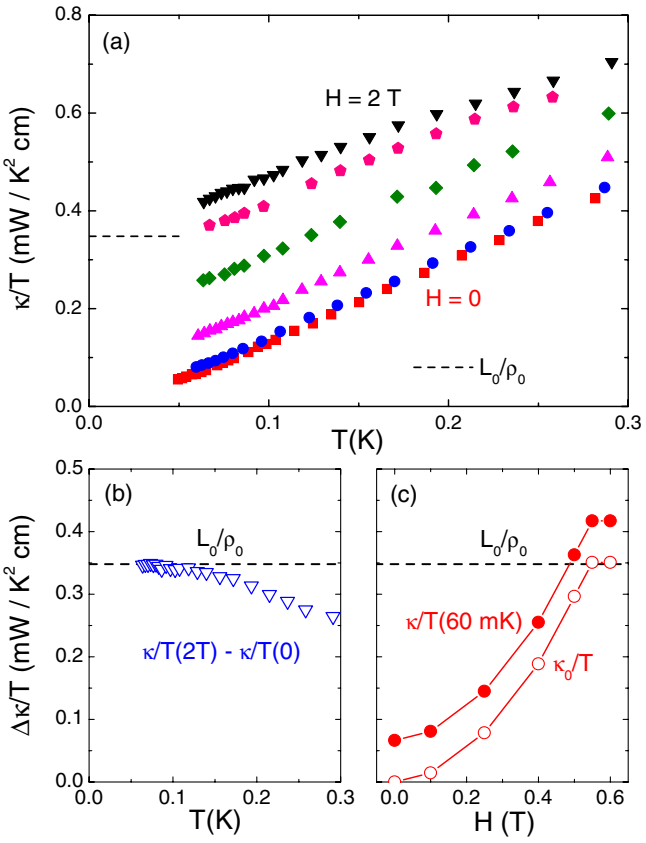

FIG. 3 (color online). (a) Low-temperature thermal conductivity of $Cu_{0.06}TiSe_2$ in magnetic fields applied along the *c* axis ($H = 0$, 0.1, 0.25, 0.4, 0.5, 2 T from bottom to top). The dashed line is the normal state Wiedemann-Franz law expectation at $T \to 0$, namely, L_0/ρ_0, with L_0 the Lorenz number 2.45×10^{-8} W Ω K^{-2}. (b) Difference in thermal conductivity between $H = 2$ T (normal state) and zero field. (c) Field dependence of κ_0/T (see text). The raw data at 60 mK is also shown.

$\kappa_0/T = L_0/\rho_0$, within 4%, which validates our method of extrapolating to $T = 0$. The same fit to the zero field data yields a negligible residual linear term, $\kappa_0/T = 0.001 \pm 0.004$ mW K^{-2} cm^{-1}, with $\alpha = 2.27$.

We can obtain a value for κ_0/T at $H = 0$ without having recourse to any fitting or extrapolation, simply by assuming that the Wiedemann-Franz law is perfectly obeyed in the normal state (at 2 T). Given that this law is universally obeyed in all good metals, this is a very reasonable assumption. In Fig. 3(b), the difference $\Delta\kappa/T = \kappa/T(2\text{ T}) - \kappa/T(0)$ is plotted. The curve saturates below about 120 mK, to a value precisely equal to L_0/ρ_0 (with ρ_0 measured on the same crystal with the same contacts). Given our assumption that $\kappa_e/T(2\text{ T}) = L_0/\rho_0$, this implies that $\kappa_e/T(0) = 0$. The fact that $\Delta\kappa/T$ is constant below 120 mK means that κ_p is the same in the superconducting state ($H = 0$) and normal state ($H = 2$ T). This indicates that electron-phonon scattering is weak in this bad metal, and it only becomes significant as T is increased (accounting for the drop in $\Delta\kappa/T$ at high T). By plotting $\Delta\kappa/T = \kappa/T(2\text{ T}) - \kappa/T(H)$ and using the same analysis, κ_0/T in fields between 0 and 2 T is obtained. The field dependence of κ_0/T is plotted in Fig. 3(c) (from which we see that the bulk $H_{c2}(0) \approx 0.55$ T). The raw data of κ/T at 60 mK are also shown.

Order parameter symmetry.—The fact that there is no residual linear term in this layered conductor, i.e., that $\kappa_0/T = 0$, directly implies that there are no nodes in the gap—the gap is nonzero everywhere on the Fermi surface. This is strong evidence in favor of an order parameter with s-wave symmetry. For unconventional superconductors with nodes in the superconducting gap, the nodal quasiparticles will contribute a finite κ_0/T in zero field. For example, $\kappa_0/T = 1.41$ mW K^{-2} cm^{-1} for the overdoped cuprate Tl2201, a d-wave superconductor with $T_c = 15$ K [15], and $\kappa_0/T = 17$ mW K^{-2} cm^{-1} for the ruthenate Sr_2RuO_4, a p-wave superconductor with $T_c = 1.5$ K [16]. The size of κ_0/T is determined by the ratio of quasiparticle velocities parallel (v_Δ) and perpendicular (v_F) to the Fermi surface near the nodes [17,18]. For a two-dimensional d-wave superconductor with a gap maximum Δ_0 and a density of n planes per unit cell of height c one gets [18]

$$\frac{\kappa_0}{T} \simeq \frac{k_B^2}{6}\frac{n}{c}\kappa_F\frac{v_F}{\Delta_0}, \qquad (1)$$

assuming $v_F \gg v_\Delta$, where k_F is the Fermi wave vector. Applying this formula to cuprate superconductors works quantitatively [19,20]. Using values appropriate for Cu_xTiSe_2, namely, $v_F = 0.4$ eV Å ($= 6.1 \times 10^4$ m/s) [21], $k_F \sim 0.5$ Å^{-1} [21], and $\Delta_0 = 2.14 k_B T_c = 0.51$ meV, Eq. (1) gives $\kappa_0/T = 2.4$ mW K^{-2} cm^{-1}. This estimate is several orders of magnitude larger than the error bar on the measured κ_0/T. Therefore we can rule out unconventional superconductivity with nodes in $Cu_{0.06}TiSe_2$. Instead, we find that the superconducting state of Cu_xTiSe_2 is characterized by a fully gapped excitation spectrum, which most likely implies an order parameter of s-wave symmetry.

Single-gap superconductivity.—In Fig. 4, the normalized κ_0/T of $Cu_{0.06}TiSe_2$ is plotted as a function of H/H_{c2}, together with similar low-temperature data for the clean s-wave superconductor Nb [22], the dirty s-wave superconducting alloy InBi [23], the multiband s-wave superconductor $NbSe_2$ [12] and an overdoped sample of the d-wave superconductor Tl-2201 [15]. For a clean type-II s-wave superconductor with a single gap, κ should grow exponentially with field (above H_{c1}), as is indeed observed in Nb [22]. For InBi, the curve is exponential at low H, crossing over to a roughly linear behavior closer to H_{c2} as expected for s-wave superconductors in the dirty limit [24]. A very similar behavior was found recently in the layered superconductor C_6Yb, whose s-wave gap was confirmed by penetration depth measurements (see Ref. [25]). However, the thermal conductivity of a multiband s-wave superconductor $NbSe_2$ [12] shows a distinctly different field dependence. In the multiband scenario, gaps of different magnitudes are associated with different bands. Applying a field rapidly delocalizes quasiparticle states confined within the vortices associated with the smaller gap band, while those states associated with the larger gap band delocalize more slowly. This gives rise to the rapid increase in κ at low fields [26] evident in the $NbSe_2$ data [12] and in the archetypal multiband superconductor MgB_2 [27]. Quantitatively, at $H = H_{c2}(0)/9$, κ_0/T in $NbSe_2$ has already risen to 1/4 of its normal-state value, while it is still negligible in a single-gap s-wave superconductor. This

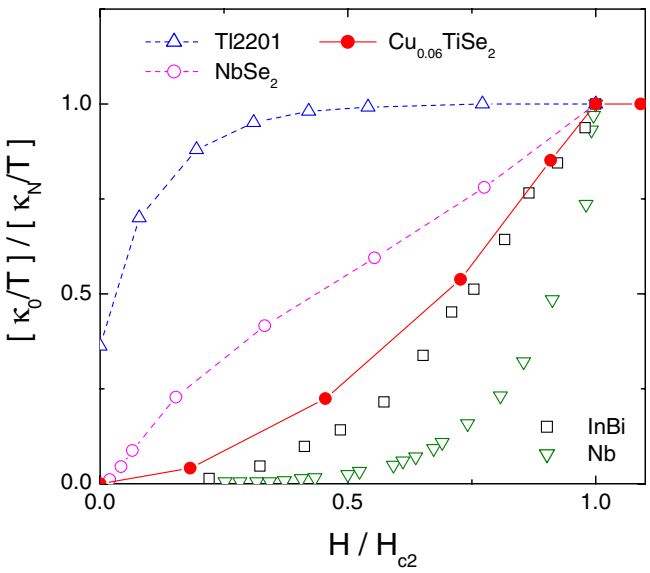

FIG. 4 (color online). Normalized residual linear term κ_0/T of $Cu_{0.06}TiSe_2$ plotted as a function of H/H_{c2}. For comparison, similar data are shown for the clean s-wave superconductor Nb [22], the dirty s-wave superconducting alloy InBi [23], the multiband s-wave superconductor $NbSe_2$ [12], and an overdoped sample of the d-wave superconductor Tl-2201 [15].

was explained in terms of a gap $\Delta_0(T \rightarrow 0)$ whose magnitude on one part of the Fermi surface is 3 times smaller than elsewhere [given that $H_{c2}(0) \propto \Delta_0^2$].

From Fig. 4, it is clear that $Cu_{0.06}TiSe_2$ is different from the multiband superconductor $NbSe_2$, and is more likely a dirty single-gap s-wave superconductor such as InBi. The BCS coherence length $\xi_0 \sim 290$ Å has been estimated from the Fermi velocity [21]. To check if $Cu_{0.06}TiSe_2$ is indeed in the dirty limit, $l < \xi_0$, we calculate the electronic mean free path l using the normal-state thermal conductivity κ_N, specific heat c, and Fermi velocity v_F. Since $\kappa_N = (1/3)cv_F l$, we get $l = 3(\kappa_N/T)/(\gamma v_F)$, where $\gamma = c/T$ is the linear specific heat coefficient. With $\kappa_N/T = 0.355\ \mathrm{mW\,K^{-2}\,cm^{-1}}$, $\gamma = 3.5\ \mathrm{mJ\,mol^{-1}\,K^{-2}}$ [1], and $v_F = 0.4$ eV Å [21], we obtain $l \sim 19$ Å, 1 order of magnitude smaller than ξ_0. This confirms $Cu_{0.06}TiSe_2$ to be in the dirty limit.

To explain the difference between the single-gap superconductivity of $1T$-Cu_xTiSe_2 and the multiband superconductivity of $2H$-$NbSe_2$, let us compare their electronic band structures. High-resolution ARPES measurements on $2H$-$NbSe_2$ [11] have shown two groups of Fermi surface (FS) sheets: a small, holelike FS centered at the Γ point derived from the Se $4p$ band and larger hexagonal FS sheets around Γ(A) and K(H) points derived from Nb $4d$ bands. Two slightly different superconducting gaps were found on the Nb $4d$ FS sheets, $\Delta = 1.0$ and 0.9 meV, respectively, while no gap was detected on the Se $4p$ FS sheet [11], at the relatively high measurement temperature of 5.3 K $= 0.74\,T_c$, in agreement with the interpretation of the κ data mentioned above [12]. It is believed that the density of states and electron-phonon coupling in the Se $4p$ band are both smaller than in the Nb $4d$ bands, which explains the difference in the magnitude of the superconducting gaps on different Fermi surfaces of $2H$-$NbSe_2$.

Previously, the Se $4p$ band in pure $1T$-$TiSe_2$ has been shown to be slightly unoccupied around Γ [6], thus a small hole pocket as in $2H$-$NbSe_2$. The Ti $3d$ band is only thermally occupied at room temperature and considerably shifts towards the occupied range upon cooling [6]. Very recently two groups have reported systematic ARPES studies of $1T$-Cu_xTiSe_2 [21,28] to explain the "competition" between CDW and superconductivity. Zhao *et al.* [28] found that, with Cu doping, the electrons will fill in the Se $4p$ hole pocket quickly and most of them are filled in the narrow Ti $3d$ band. Since the Se $4p$ band is fully occupied in $1T$-$Cu_{0.06}TiSe_2$, there is only the Ti $3d$ band responsible for superconductivity. This explains why $1T$-$Cu_{0.06}TiSe_2$ is a single-gap superconductor, different from the multiband superconductor $2H$-$NbSe_2$.

Based on their study, Zhao *et al.* [28] concluded that the apparent competition between CDW and superconductivity in $1T$-Cu_xTiSe_2 is very likely a coincidence, as the doping will increase the density of states (enhance SC) and raise the chemical potential (suppress CDW according to the excitonic mechanism originally proposed by Kohn [29]) simultaneously. And the drop of superconductivity at high doping might be due to strong scattering caused by the dopants. In this sense, it may not come as a surprise that we observe conventional superconductivity in this system. In other words, the appearance of superconductivity may have little to do with the suppression of CDW order and associated fluctuations.

In summary, we have used thermal conductivity to clearly demonstrate single-gap s-wave superconductivity in $Cu_{0.06}TiSe_2$. This rules out unconventional superconductivity with gap nodes in Cu_xTiSe_2, despite the quantum phase transition from CDW order to superconductivity induced by Cu doping. In contrast to the multiband s-wave superconductor $NbSe_2$, our result implies that the Se $4p$ band in $Cu_{0.06}TiSe_2$ is below the Fermi level and Cu doping into the Ti $3d$ band is responsible for superconductivity, in agreement with ARPES studies.

We are grateful to P. Fournier for sample characterization. This research was supported by NSERC of Canada, a Canada Research Chair (L. T.), and the Canadian Institute for Advanced Research. The work in China was supported by a grant from the Natural Science Foundation of China.

*louis.taillefer@usherbrooke.ca

[1] E. Morosan *et al.*, Nature Phys. **2**, 544 (2006).
[2] N. D. Mathur *et al.*, Nature (London) **394**, 39 (1998).
[3] H. Q. Yuan *et al.*, Science **302**, 2104 (2003).
[4] P. Monthoux and G. G. Lonzarich, Phys. Rev. B **69**, 064517 (2004).
[5] J. A. Wilson *et al.*, Adv. Phys. **24**, 117 (1975).
[6] Th. Pillo *et al.*, Phys. Rev. B **61**, 16 213 (2000).
[7] T. E. Kidd *et al.*, Phys. Rev. Lett. **88**, 226402 (2002).
[8] T. Valla *et al.*, Phys. Rev. Lett. **92**, 086401 (2004).
[9] R. L. Barnett *et al.*, Phys. Rev. Lett. **96**, 026406 (2006).
[10] A. H. Castro Neto, Phys. Rev. Lett. **86**, 4382 (2001).
[11] T. Yokoya *et al.*, Science **294**, 2518 (2001).
[12] E. Boaknin *et al.*, Phys. Rev. Lett. **90**, 117003 (2003).
[13] G. Wu and X. H. Chen Phys. Rev. B **76**, 024513 (2007).
[14] E. Morosan *et al.*, Phys. Rev. B **75**, 104505 (2007).
[15] C. Proust *et al.*, Phys. Rev. Lett. **89**, 147003 (2002).
[16] M. Suzuki *et al.*, Phys. Rev. Lett. **88**, 227004 (2002).
[17] M. J. Graf *et al.*, Phys. Rev. B **53**, 15 147 (1996).
[18] A. C. Durst and P. A. Lee, Phys. Rev. B **62**, 1270 (2000).
[19] May Chiao *et al.*, Phys. Rev. B **62**, 3554 (2000).
[20] D. G. Hawthorn *et al.*, Phys. Rev. B **75**, 104518 (2007).
[21] D. Qian *et al.*, Phys. Rev. Lett. **98**, 117007 (2007).
[22] J. Lowell and J. Sousa, J. Low Temp. Phys. **3**, 65 (1970).
[23] J. Willis and D. Ginsberg, Phys. Rev. B **14**, 1916 (1976).
[24] C. Caroli *et al.*, Phys. Kondens. Mater. **4**, 285 (1965).
[25] M. Sutherland *et al.*, Phys. Rev. Lett. **98**, 067003 (2007).
[26] H. Kusunose *et al.*, Phys. Rev. B **66**, 214503 (2002).
[27] A. V. Sologubenko *et al.*, Phys. Rev. B **66**, 014504 (2002).
[28] J. F. Zhao *et al.*, arXiv:cond-mat/0612091.
[29] W. Kohn, Phys. Rev. Lett. **19**, 439 (1967).